International Journal of Railway Research, Vol. 13, No. 1, (2026), 37-51

Iran University of Science and Technology

International Journal of

Railway Research

ISSN: 2423-3838

Evaluation of Axle Stress in Y25 and 18-100 Bogies during Curve Negotiation: A Comparative Study Using Multibody Dynamics and Finite Element Analysis

Seyed Mohammad Reza Mousavi [1], Amin Owhadi [2*], Majid Shahravi [3]

[1] Graduate in Railway Engineering, Faculty of Railway Engineering, Iran University of Science and Technology

[2] Assistant Professor of Railway Engineering, Iran University of Science and Technology

[3] Associate Professor of Railway Engineering, Iran University of Science and Technology

ARTICLE INFO

Article history:

Received: (TNR 9 Regular)

Accepted: 00.00.0000

Published: 00.00.0000

Keywords:

Stress Analysis

Railway Axle

Freight Bogie

Y25 Bogie

18-100 Bogie

Curve Negotiation

Finite Element Analysis (FEA)

Multi-Body Dynamics (MBD)

A B S T R A C T

Railway axles are safety-critical components whose structural integrity is paramount, especially under dynamic loads encountered during curve negotiation, where fatigue cracking often initiates at press-fitted components. This study presents a comparative stress analysis of the axles in two widely used freight bogies, the Y25 and the 18-100, while traversing curved tracks. A combined simulation methodology was employed: dynamic forces were first extracted using Multibody Dynamics (MBD) analysis in Universal Mechanism (UM) software. These forces were then applied to detailed finite element models of the axles, developed in CATIA and analyzed in Abaqus, to determine the stress distributions. The analysis was performed for curve radii of 400 m and 1000 m at speeds of 72, 90, and 108 km/h. Results indicate that the maximum von Mises stress occurs at the fillet region between the axle journal and the wheel seat (Section A), predominantly on the outer axle. The 18-100 bogie axle experienced a higher maximum stress (357.57 MPa) compared to the Y25 bogie axle (248.33 MPa) under the most critical condition (400 m curve at 108 km/h). Stress magnitudes increased significantly with speed on sharper curves, highlighting the critical influence of operational parameters. The findings provide valuable insights for bogie selection, maintenance planning, and future design optimizations, such as the potential use of composite materials to reduce weight and mitigate fatigue.

1. Introduction

The structural dynamics of railway bogies significantly influence vehicle safety, operational performance, and maintenance requirements. As fundamental bogie components, axles represent critical safety elements whose failure can lead to catastrophic consequences. Despite advancements in fatigue design methodologies, the risk of crack initiation at press-fitted components remains a persistent concern, necessitating rigorous inspection protocols and continuous structural assessment [1].

Curve negotiation presents one of the most demanding loading conditions for railway axles, particularly in urban rail systems characterized by tight curves with small radii. During curve traversal, complex wheel-rail interaction mechanisms induce substantial stresses on both track and bogie components, leading to accelerated wear, elevated noise levels, and accelerated fatigue damage primarily driven by unfavorable attack angles and elevated creepages at the wheel-rail interface [2,3].

The axle has three main sections: the journal (J), the wheel seat (B), and the main section of the axle (A) located between two wheels. The

*Corresponding author
Email address: aohadi@iust.ac.ir

wheel seat is a part of the axle that fits into the wheel body in a wedge-shaped configuration.

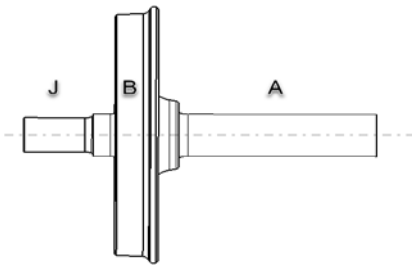

Figure 1. Three main sections of an axle.

Previous research has established foundational knowledge in this domain. Torstensson and Nielsen [2] investigated vehicle-track interaction on small-radius curves using GENSYS software, while Tuna et al. [3] examined wear and rolling contact fatigue mechanisms. Wang et al. [4] comprehensively reviewed wheel-rail dynamics during curve negotiation, and Wu et al. [5] developed advanced vehicle/track models to study polygonal wear effects. Parallel studies by Beretta [6], Madia [7], and Hirakawa [8] have addressed fatigue performance and crack growth in railway axles under various loading conditions.

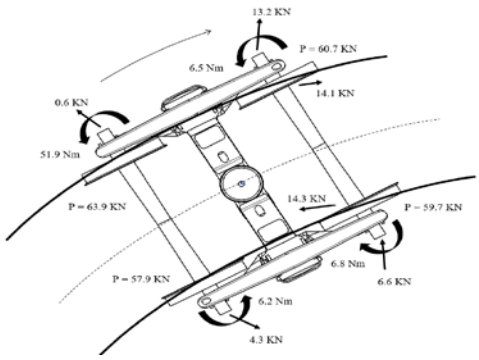

Figure 2. Common forces on the wheels when passing through a curve.

Among various bogie designs employed in freight operations, the 18-100 bogie has been extensively utilized in broad-gauge networks since the 1950s, undergoing numerous design refinements over decades of service. Conversely, the Y25 bogie has gained prominence in narrow-gauge applications due to its favorable operational characteristics and recent design improvements [5]. A comparative analysis of dynamic loading and stress behavior between these two bogie types can provide valuable insights for bogie selection and optimization.

The dynamic performance of wheel-rail interactions on curved tracks has constituted a significant research focus in train dynamics, yielding numerous theoretical and experimental investigations internationally. Four primary research domains have emerged: (1) mechanisms and computational methods for curve negotiation, (2) analysis and evaluation of rolling stock dynamic performance, (3) influence of vehicle parameters on dynamic behavior, and (4) impact of railway parameters on dynamic performance [4]. Recent studies have further explored the dynamic interaction between freight car bodies and bogies under increased axle loads [10, 13] and the use of advanced instrumentation for stress-strain analysis [14], highlighting the complex load transfer mechanisms that influence axle stress states.

However, a systematic comparison of stress distributions in Y25 and 18-100 bogie axles under identical operational scenarios remains unexplored. This research gap is addressed herein through an integrated simulation approach combining multi-body dynamics and finite element analysis. The study aims to: (1) quantify dynamic forces acting on bogie axles during curve negotiation at various speeds and curve radii, (2) compare stress distributions and identify critical locations in Y25 and 18-100 bogie axles, and (3) establish correlations between operational parameters and stress magnitudes to provide foundational data for bogie design optimization and maintenance planning.

2. Research Methodology

2.1. Overall Approach

This study employs an integrated computational methodology combining multibody dynamics (MBD) and finite element analysis (FEA) to evaluate axle stresses in Y25 and 18-100 bogies. The research framework

comprises three sequential phases: (1) dynamic force extraction using MBD simulation, (2) finite element modeling of bogie axles, and (3) stress analysis and comparative evaluation.

2.2. Modeling and Evolution

Three-piece bogies are used due to their simplicity in design, ease of construction, and ability to bear more load in freight transport. This research aims to examine the stresses on the axles of two models of these freight bogies as they pass through curves with different radii at varying speeds.

2.3. Wheelset in a Curve

Let us consider a free wheelset (without a suspension system) with conical profiles. We assume pure rolling, meaning no creeps at the contact point. Furthermore, no centrifugal force is applied to the wheelset.

To achieve radial steering, as shown in Figure 3, due to the conical shape of the wheels, a difference in the radius of rotation of the wheels occurs, causing one wheel to advance ahead of the other. The outer wheel must rotate over a longer distance compared to the inner wheel. This is possible only if the wheelset shifts outward along the curve, allowing the outer wheel to rotate at a larger radius than the inner wheel. The required ratio between the outer and inner curve radii is referred to here as the rolling line, which can be calculated as follows.[1].

$$\frac{r_{out}}{r_{in}} = \frac{R+e_0}{R-e_0} \quad (1)$$

where it is assumed $e_0 = e_i = e_a$. for conical profiles.

$$r_{out} = r_0 + \delta_0 u_y \quad (2)$$

$$r_{in} = r_0 - \delta_0 u_y \quad (3)$$

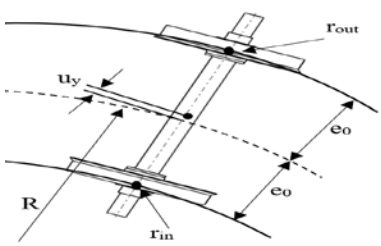

Figure 3. Radial steering of a free wheelset with conical profiles in a curve.

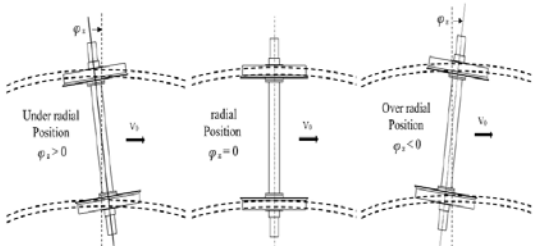

Figure 4. Possible positions of the wheel on the path.

Equations (2) and (3) were substituted into (1), resulting in lateral wheel displacement.

$$u_y = \frac{r_0 e_0}{\delta_0 R} \quad (4)$$

The lateral displacement required for radial steering decreases further with increased arc radius R and conicity δ_0. Previously, a contrast with movement along a straight path was demonstrated here. For the curve, following equation (4), a high conicity δ_0 is advantageous. In contrast, low conicity is preferred for stability in straight-line movement. Suppose the required rolling radius difference cannot be achieved. As shown in Figure 4, the wheelset suspended in a bogie assumes a radial or sub-radial position [1].

2.4. Simulation of Freight Wagon Dynamics

In this paper, the UM software was used for dynamic simulation. In the freight wagon model with bogies 18-100 and Y25, the actual values of the distance between the axle box and the bogie frame, and between the support and the frame were considered. The freight wagon was modeled as a rigid body with actual dimensions, mass, and center of mass position.

The carbody is modeled as a rigid body. Additionally, a constant coefficient of friction at the center pivot (default value) is assumed without sensitivity analysis. While this simplification is acceptable for comparative purposes, the absolute load distribution in the three-piece bogie (18-100) may be influenced by the actual friction condition, which varies with wear and lubrication. Future work should

include a sensitivity study on the friction coefficient (e.g., 0.1–0.5) and consider flexible carbody torsion stiffness.

2.5. Multi-Body Dynamics Simulation

The dynamic behavior of freight wagons equipped with Y25 and 18-100 bogies was simulated using Universal Mechanism (UM[1]) software. The wagon was modeled as a rigid body with actual mass properties and geometric dimensions. Both bogie types were modeled according to their technical specifications, incorporating actual values for suspension parameters, axle box arrangements, and structural configurations.

Simulations were conducted for curved tracks with radii of 400 m and 1000 m, each with a length of 600 m, at operating speeds of 72, 90, and 108 km/h. The track was modeled without irregularities to isolate the effects of curve negotiation. The output from these simulations included time-history data of forces and moments transmitted from the track to the axle in three orthogonal directions (lateral, longitudinal, and vertical).

The validity of the multibody dynamics modeling approach was supported by comparisons with established methodologies in the literature, particularly concerning the simulation of freight wagon dynamics on curved tracks [10, 11, 17]. These studies confirm the applicability of MBD simulations for capturing the essential dynamic forces required for subsequent stress analysis.

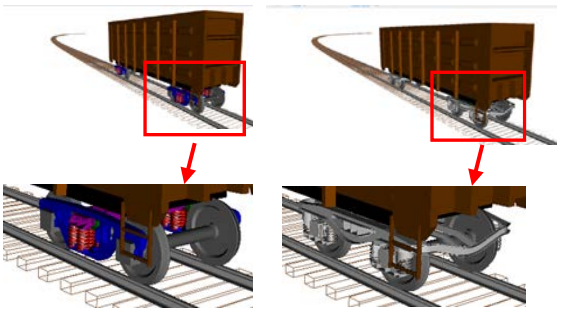

a) b)

Figure 5. a) Bogie 18-100 and b) Y25 on a curved track.

The Y25 and 18-100 bogies were designed and modeled in the CATIA platform. They were then transferred to the Abaqus simulation platform for stress analysis and evaluation. The simulations were based on real measurements according to the drawings of these two bogies.

a)

b)

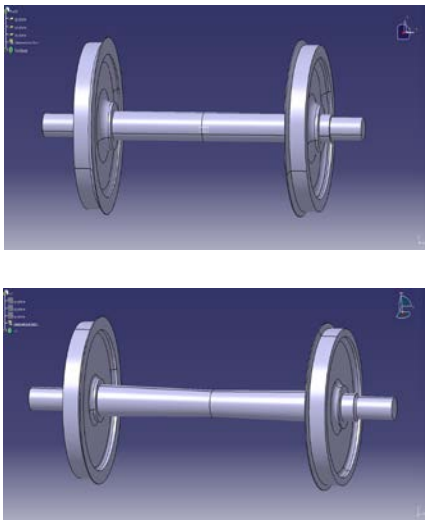

Figure 6. Designed wheel and axle of bogie, a) Y25 and b) 18-100 in the Catia platform.

2.6. Finite Element Modeling

The finite element approach for simulating wheel-rail contact response, especially for curved tracks, is well-established and has been successfully implemented in prior research to analyze complex contact mechanics and stress distributions [15].

Detailed three-dimensional models of both bogie axles were developed in CATIA V5, adhering to manufacturer specifications and technical drawings. The models were imported into Abaqus/CAE for finite element analysis. The axle material was modeled as high-strength railway steel with the following properties: Young's modulus = 210 GPa, Poisson's ratio = 0.3, and Yield stress = 545 MPa.

The load should provide a realistic stress-strain condition across all model elements. Load values are obtained from the dynamic simulation (UM). For the wheel and axle, the forces applied from

[1] Universal Mechanism

the track to the wheels and from the bogie frame to the axle, and their time variation is determined by the loads set on the freight wagon. Load values from the dynamic simulation of the freight wagon under various conditions were extracted from the UM software. In each case, a wagon with a specified mass moves at a certain speed along a defined curved path. It was assumed that the relative positions of the bodies do not affect the distribution of contact stresses, and the contact stresses were calculated for the initial positions of the bodies.

2.7. Meshing and Convergence

A hex-dominant meshing strategy was employed to balance computational efficiency and accuracy. Mesh sensitivity analysis was conducted to ensure result convergence. The final models contained 74,386 elements for the 18-100 axle and 81,887 elements for the Y25 axle, at which point stress results stabilized within 2% variation.

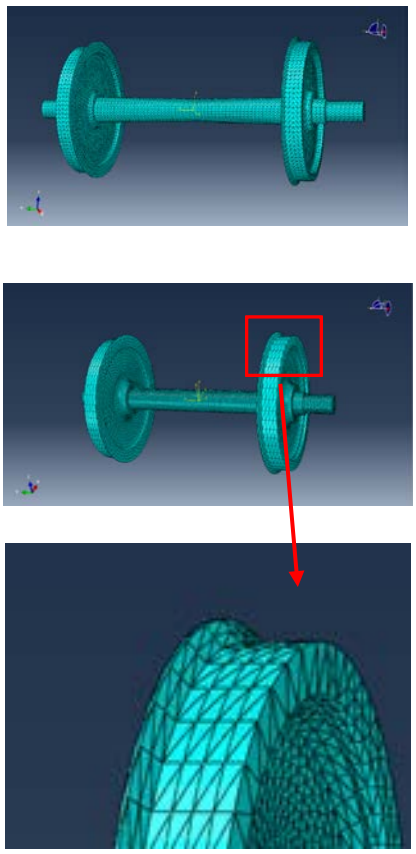

Figure 7. Meshing of wheel and axle 18-100 and Y25.

2.8. Load Application and Boundary Conditions

Forces obtained from MBD simulations were applied to FE models as static load cases representing peak dynamic conditions. Loading included forces from the bogie frame onto the axle and reaction forces from wheel-rail interaction. The von Mises stress criterion was employed for stress evaluation due to its appropriateness for ductile metals under multiaxial loading.

It should be noted that the current approach applies the peak dynamic forces as static loads without simulating the rotation of the axle relative to the wheel. Consequently, the cyclic bending stress at the fillet region (Section A) due to axle rotation is not captured, which may lead to an underestimation of actual peak stresses by approximately 20–30% compared to service conditions. Nevertheless, the comparative assessment between the two bogie axles remains valid as both models share the same simplification.

However, due to using average force values from MBD outputs, the high-frequency fluctuations of longitudinal force (see standard deviations in Tables 1 and 2) – which arise from stick-slip transitions during curve negotiation – are not transferred to the FE model. Consequently, the alternating shear stresses at the fillet region are not fully represented. This limitation may lead to non-conservative fatigue life estimates and should be addressed in future studies through transient dynamic analysis.

3. Results and Discussion

In this chapter, using the UM Simulation platform, the dynamic forces during the passage through the curve were extracted, and by inputting these results into the Abaqus program and obtaining the stresses, a comparison was made.

The developed models of freight wagons allow for obtaining fundamental dynamic performance metrics such as derailment coefficients, lateral track shifting forces, wear factors, contact stresses, ride comfort, acceleration of any point on the body, and other performances in tangent paths and curves; adjusting inertia and geometric parameters, spring and damper parameters, and

acquiring the dynamic behavior of the wagon using different rail and wheel profiles while tracking irregularities, enabling the demonstration of the derailment process and wheel lift.

3.1. Dynamic Force Analysis

Initially, we placed both bogie models on a high-sided wagon and passed them through a curved path without irregularities, with curve radii of 400 and 1000 meters along a path length of 600 meters at speeds of 72, 90, and 108 kilometers per hour, then obtained the dynamic analyses for each. In this section, results and explanations about each of the dynamic analyses are provided first.

The dynamic forces acting on the wheel and axle stem from the frame of the bogie on the wheel and axle and the forces exerted by the path. These applied forces were obtained in all three directions: x, y, and z. After analyzing and comparing them, the average force obtained during motion was used for stress analysis and comparison in Abaqus.

The MBD simulations revealed distinct force patterns between the two bogie types. Figure 8. illustrates representative force-time histories for both bogies negotiating a 400 m curve at 108 km/h. Consistent with theoretical expectations, the outer wheels experienced significantly higher lateral and vertical forces compared to inner wheels, with the 18-100 bogie showing more pronounced load variations.

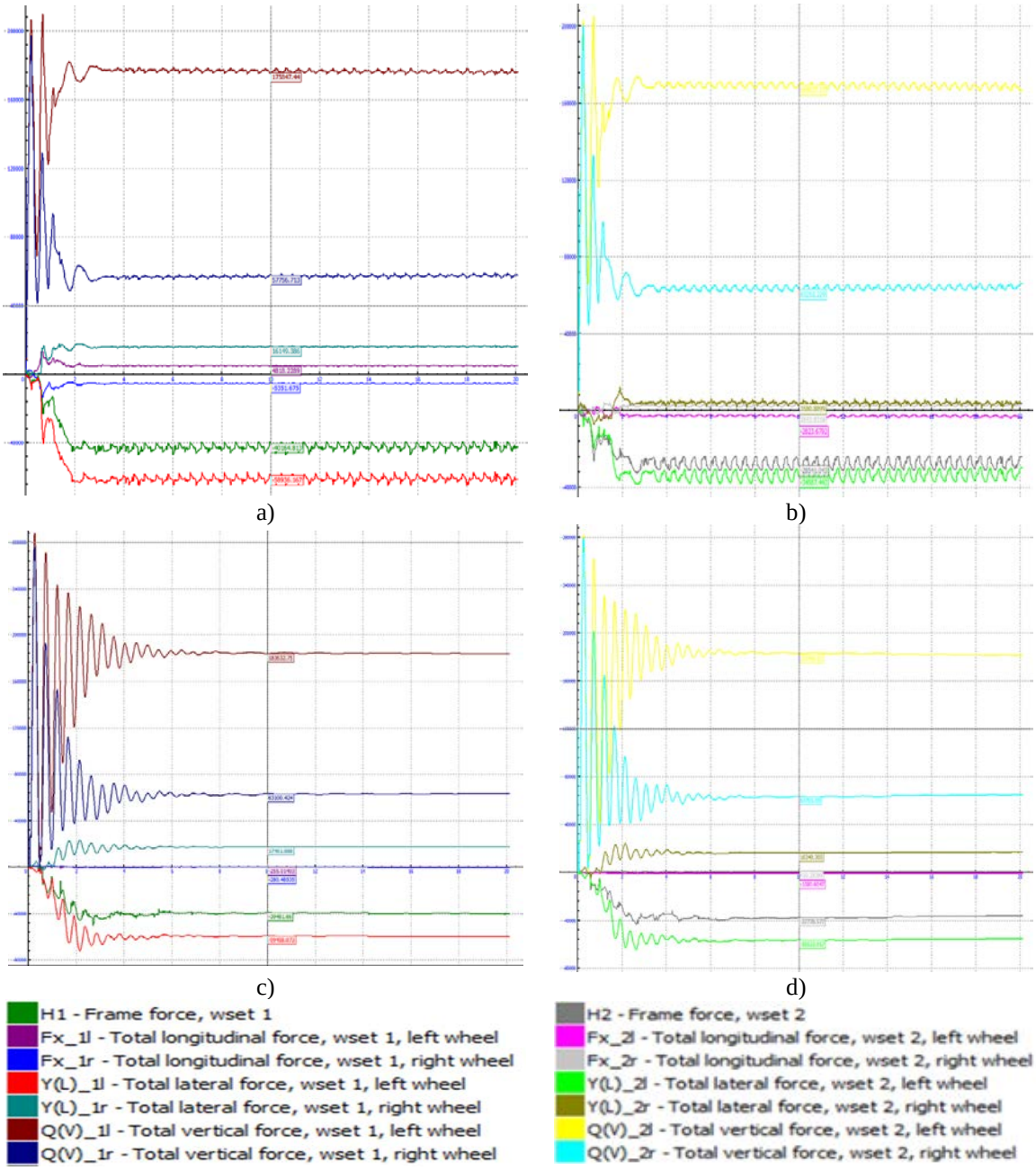

Figure 8. force (N) versus time (s) for (a) the front wheel and axle, (b) the rear wheel and axle of bogie 18-100, (c) the front wheel and axle, and (d) the rear wheel and axle of bogie Y25 in a curve with a radius of 400 meters and a speed of 108 kilometers per hour.

Table 1. maximum, minimum, and average dynamic forces along with the standard deviation and sample length for both the wheels and axle of bogie 18-100 in a curve with a radius of 400 meters and a speed of 108 kilometers per hour.

Variables	Length of sample (m)	Mean (N)	StdDev	Min (N)	**Max (N)**
Frame force, wset 1	1005	-40302.88	8472.129	-46782.98	**357.919**
Total longitudinal force, wset 1, left wheel	1005	4983.484	1207.096	-2206.301	**13948.12**
Total longitudinal force, wset 1, right wheel	1005	-5497.669	1293.746	-13677.41	**9683.293**
Total lateral force, wset 1, left wheel	1005	-57950.4	11447.61	-65426.21	**-142.2673**
Total lateral force, wset 1, right wheel	1005	15320.51	2808.683	-387.1083	**17847.16**
Total vertical force, wset 1, left wheel	1005	174250.4	13948.93	8603.417	**209691.9**
Total vertical force, wset 1, right wheel	1005	59422.28	13337.15	9456.148	**197270.8**
Frame force, wset 2	1005	-26157.71	5448.11	-32218.12	**3160.05**
Total longitudinal force, wset 2, left wheel	1005	-2591.198	858.0261	-4234.521	**2044.754**
Total longitudinal force, wset 2, right wheel	1005	2476.758	820.6501	-1650.43	**9683.293**
Total lateral force, wset 2, left wheel	1005	-32003.21	7035.577	-38370.18	**-16.26**
Total lateral force, wset 2, right wheel	1005	3561.273	2062.245	-7242.633	**12327.25**
Total vertical force, wset 2, left wheel	1005	166698.3	13307.92	8336.516	**205224.5**
Total vertical force, wset 2, right wheel	1005	66079.76	12920.39	9725.291	**200510.9**

Table 2. maximum, minimum, and average dynamic forces along with the standard deviation and sample length for both the wheels and axle of bogie Y25 in a curve with a radius of 400 meters and a speed of 108 kilometers per hour.

Variables	Length of sample (m)	Mean (N)	StdDev	Min (N)	**Max (N)**
Frame force, wset 1	1007	-37935.31	8048.131	-50086.75	**399.9503**
Total longitudinal force, wset 1, left wheel	1007	-228.5809	79.5349	-730.4508	**358.7698**
Total longitudinal force, wset 1, right wheel	1007	-247.2136	149.8446	-538.0663	**586.0424**
Total lateral force, wset 1, left wheel	1007	-56587.97	12157.91	-71997.14	**0**
Total lateral force, wset 1, right wheel	1007	16228.52	4013.399	-4145.903	**23273.54**
Total vertical force, wset 1, left wheel	1007	181189.3	27439.17	0	**287708.3**
Total vertical force, wset 1, right wheel	1007	65512.45	23727.68	0	**275486.2**
Frame force, wset 2	1007	-35036.37	8074.359	-43332.74	**97.78445**
Total longitudinal force, wset 2, left wheel	1007	-1029.556	202.8186	-1828.117	**0**
Total longitudinal force, wset 2, right wheel	1007	614.1489	92.08072	-119.2303	**1143.236**
Total lateral force, wset 2, left wheel	1007	-52775.85	12035.84	-64568.94	**172.9599**
Total lateral force, wset 2, right wheel	1007	15358.4	3866.316	-5148.052	**23994.33**
Total vertical force, wset 2, left wheel	1007	179039.4	27626.72	0	**282213.1**
Total vertical force, wset 2, right wheel	1007	67177.77	24555.96	0	**278751.8**

The significant standard deviations of longitudinal forces (e.g., ~1200 N for 18-100 bogie at 108 km/h) indicate intermittent stick-slip behavior, which is not captured in the subsequent static FE analysis.

Quantitative analysis of force distributions (Tables 1 and 2) demonstrated that:

- Vertical forces dominated the loading regime, particularly on the outer wheel.
- Lateral forces increased progressively with speed on sharper curves.
- The 18-100 bogie transmitted approximately 25-30% higher forces to its axles compared to the Y25 bogie under identical conditions.

The maximum dynamic forces acting on the wheels and axle of the bogies while passing through a curve is the total of the vertical forces, followed by the total of the lateral forces acting on the left and right wheels of the axle.

In the 18-100 bogie at a 400-meter curve, the total longitudinal forces acting on both the right and left wheels decrease by 400 Newtons for every 5 kilometers per hour increase in speed. However, the left wheel's total vertical and lateral forces increase due to pressure and contact with the outer rail while passing through the curve. The total lateral forces acting on the left wheel increase by 6 KN with an increase in speed from 72 to 90 kilometers per hour, and by 11 KN with an increase in speed from 90 to 108 kilometers per hour. The total vertical forces acting on the left wheel increase by 2 KN for every 18 kilometers per hour increase in speed. Conversely, the total vertical and lateral forces on the right wheel decrease due to reduced pressure and contact with the inner rail while passing through the curve. Specifically, the total lateral forces acting on the right wheel decrease by 5 KN for every 18 kilometers per hour increase in speed, and the total vertical forces on the right wheel decrease by 16.6 KN when speed increases from 72 to 90 kilometers per hour, and by 21.7 KN when speed increases from 90 to 108 kilometers per hour.

In the bogie 18-100 on a 1000-meter curve, the total longitudinal, lateral, and vertical forces on the left wheel increase with increasing speed, while the total lateral and vertical forces on the right wheel decrease with increasing speed.

On the left wheel, for every 18 kilometers per hour increase in speed, the total longitudinal, lateral, and vertical forces increase by approximately 400 N, 4 KN, and 8 KN respectively. For the right wheel, the total lateral forces decrease by 1.7 KN when speed increases from 72 to 90 kilometers per hour, and by 3.2 KN when speed increases from 90 to 108 kilometers per hour. The total vertical forces on the right wheel decrease by 7.2 KN when speed increases from 72 to 90 kilometers per hour, and by 9.7 KN when speed increases from 90 to 108 kilometers per hour.

In the Y25 bogie, during a 400-meter curve, the total longitudinal forces acting on both the left and right wheels do not change significantly with increasing speed and have a very minor impact due to their low magnitude. However, the total vertical and lateral forces on the left wheel increase due to pressure and contact with the outer rail while navigating the curve, whereas they decrease on the right wheel. The total lateral forces on the left wheel increase by 5.5 KN when speed rises from 72 to 90 kilometers per hour, and by 8.2 KN when speed increases from 90 to 108 kilometers per hour. The total vertical forces on the left wheel increase by 14.9 KN when speed goes from 72 to 90 kilometers per hour, and by 24.5 KN when speed increases from 90 to 108 kilometers per hour. The total lateral forces on the right wheel decrease by 3.8 KN when speed rises from 72 to 90 kilometers per hour, and by 6 KN when speed increases from 90 to 108 kilometers per hour. Additionally, the total vertical forces on the right wheel decrease by 14.4 KN when speed goes from 72 to 90 kilometers per hour, and by 24.6 KN when speed increases from 90 to 108 kilometers per hour.

In a 1000-meter curve, the left wheel's total lateral and vertical forces increase with speed, while the total lateral and vertical forces on the right wheel decrease.

For the left wheel, the total lateral forces increase with an increase in speed from 72 to 90 kilometers per hour by 1.7 KN, and from 90 to 108 kilometers per hour by 3.3 KN. The total vertical forces increase with an increase in speed from 72 to 90 kilometers per hour by 6.3 KN, and from 90 to 108 kilometers per hour by 9.4 KN. For the right wheel, the total lateral forces decrease with an increase in speed from 72 to 90 kilometers per hour by 1.3 KN and decrease from 90 to 108 kilometers per hour by 4.9 KN.

The total vertical forces decrease with an increase in speed from 72 to 90 kilometers per hour by 6 KN, and from 90 to 108 kilometers per hour by 9 KN.

According to the conducted analysis, the main dynamic force acting during the passage through the curve is the total vertical forces transmitted from the track to the wheels, which is particularly noticeable on the left wheel due to increased pressure and contact with the outer rail.

3.2. Stress Distribution and Critical Locations

Finite element analysis identified consistent stress concentration at the fillet region between the axle journal and wheel seat (Section A), as depicted in Figure 9. This location corresponds to typical fatigue-critical zones identified in railway axle failures.

For the 18-100 bogie axle, the maximum average stress reached 357.57 MPa under the most severe condition (400 m curve at 108 km/h). The Y25 bogie axle showed superior performance with a maximum stress of 248.33 MPa under identical conditions, representing a 30% reduction that suggests better force distribution characteristics in the Y25 design. The identified critical location and stress patterns align with findings from static and dynamic testing of bogie components [11] and reviews of wheel-rail dynamic behavior on curved tracks [16].

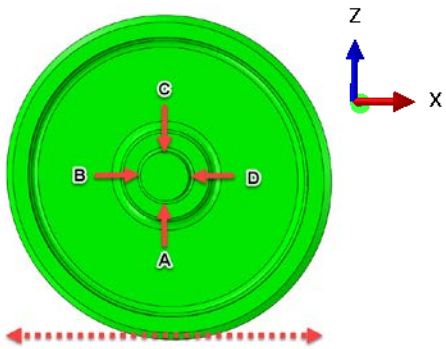

Figure 9. location of stress analysis on the axle.

The von Mises stress distribution around the fillet circumference (Section A) was not extracted in the present study due to the static loading assumption. However, based on the direction of the resultant lateral and vertical forces, the peak stress is expected to occur at the angular position aligned with the resultant bending moment. The approximately 44% higher peak stress in the 18-100 axle compared to the Y25 axle, despite similar vertical loads, is primarily attributed to the smaller fillet radius (higher stress concentration factor) and the significantly larger longitudinal force component in the 18-100 bogie (see Tables 1 and 2). Mesh sensitivity analysis confirmed convergence within 2%, so numerical interpolation errors are not the main cause.

3.2.1. Stress Analysis of Axle 18-100

This section analyzes the stresses on axle 18-100 in curves with radii of 400 and 1000 meters at speeds of 72, 90, and 108 kilometers per hour.

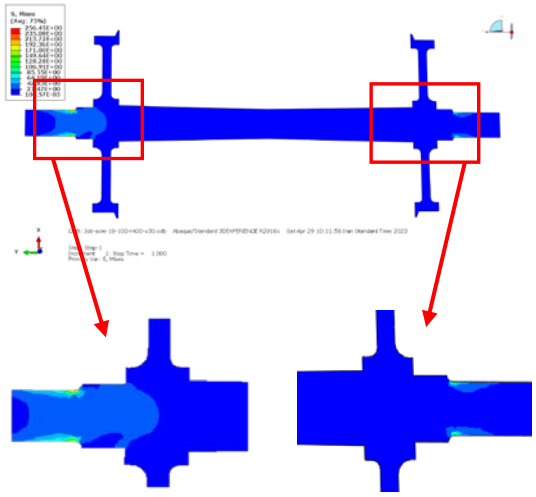

Figure 10. Stress applied to the wheel and axle of bogie 18-100 while passing through a curve with a radius of 400 meters at a speed of 108 kilometers per hour.

The average stresses on the wheels and axle 18-100 in the 400-meter curve increase by 6.8% as the speed rises from 72 km/h to 90 km/h, and by 15.4% as the speed increases from 90 km/h to 108 km/h. In the 1000-meter curve, the average stresses decrease by 6% as the speed rises from 72 km/h to 90 km/h and by 8.6% as the speed increases from 90 km/h to 108 km/h. The difference in average stresses on the wheels and axle 18-100 in the 400 and 1000-meter curves at speeds of 72 km/h, 90 km/h, and 108 km/h is 21.8%, 7.2%, and 17.7%, respectively.

Table 3. Average stress (MPa) applied to the axle of bogie 18-100.

Speed (km/h)	400 (m) curve							
	External axle				Internal axle			
	A	B	C	D	A	B	C	D
72	293.67	173.67	109.14	215.82	251.62	184.39	84.45	135.58
90	293.12	191.93	121.47	231.48	231.52	166.64	78.24	121.94
108	357.57	218.22	136.65	256.44	211.60	147.84	79.90	105.75
	1000 (m) curve							
72	195.02	116.22	74.28	179.41	219.47	192.26	79.95	124.65
90	214.53	124.02	79.84	190.28	215.38	188.28	78.07	117.99
108	230.52	133.80	85.65	201.41	204.03	179.74	74.05	109.00

The average stress on the axle is observed at the fillet at the intersection between the axle head and the wheel disc. The maximum average stress is mainly found in the fillet located under the intersection between the axle head and the left wheel disc, due to the increase in force with increasing speed and decreasing curve radius. The maximum average stress in the 400-meter curve at a speed of 108 km/h is 357.57 MPa, while the maximum average stress in the 1000-meter curve at the same speed is 230.52 MPa, occurring on the external axle at section A.

It should be noted that the slight decrease in stress from 72 to 90 km/h on the outer axle of the 18-100 bogie (equivalent to 0.19%, within the range of numerical fluctuations of the dynamic simulation given the force standard deviations in Table 1) has no physical significance and does not violate the overall increasing trend of stress with speed. The critical peak stress under all conditions occurs at 108 km/h.

3.2.2. Stress analysis of axle Y25

This section also analyzes the stresses on axle Y25 in curves with radii of 400 and 1000 meters at speeds of 72, 90, and 108 kilometers per hour.

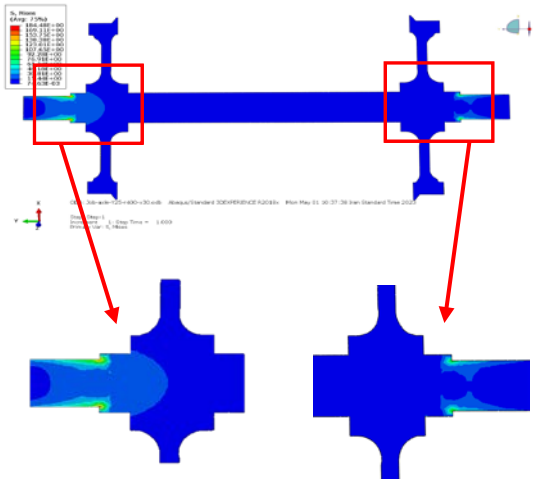

Figure 11. Stress applied to the wheel and axle of bogie Y25 while passing through a curve with a radius of 400 meters at a speed of 108 kilometers per hour.

The average stresses applied to the Y25 wheel and axle in a 400-meter curve increase by 10.7% when speed rises from 72 km/h to 90 km/h and by 15.7% when speed increases from 90 km/h to 108 km/h. In a 1000-meter curve, the average stresses increase by 3.6% with a speed increase from 72 km/h to 90 km/h and by 7.5% when speeding up from 90 km/h to 108 km/h. The difference in average stresses applied to the Y25 wheel and axle in the 400 and 1000-meter curves at speeds of 72 km/h, 90 km/h, and 108 km/h are 18.3%, 26.4%, and 36.1%, respectively.

Table 4. Average stress (MPa) applied to the axle of bogie Y25.

Speed (km/h)	400 (m) curve							
	External axle				Internal axle			
	A	B	C	D	A	B	C	D
72	209.32	130.91	77.59	141.15	204.00	104.13	67.22	114.08
90	224.64	165.75	83.09	151.92	191.10	118.44	63.21	105.24
108	248.33	184.48	91.52	169.07	169.02	101.59	56.36	89.97
	1000 (m) curve							
72	133.35	108.96	57.32	102.57	160.88	115.43	56.99	101.73
90	138.88	113.44	60.38	106.91	155.61	111.40	49.19	97.87
108	146.85	120.60	62.99	111.87	141.72	101.98	44.59	91.12

The average stress applied to the axle can be observed at the fillet of the intersection between the axle head and the wheel disk. The maximum average stress is primarily found in the fillet under the intersection between the axle head and the left wheel disk due to the increased forces with the increase in speed and the decrease in the radius of the curve. The maximum average stress in the 400-meter curve at a speed of 108 km/h is 248.33 MPa, and the maximum average stress in the 1000-meter curve at a speed of 72 km/h is 160.88 MPa on the external axle in section A.

3.2.3. Comparison of Axles

In this section, we have compared both bogie Axles with each other using the results of the analyses mentioned above.

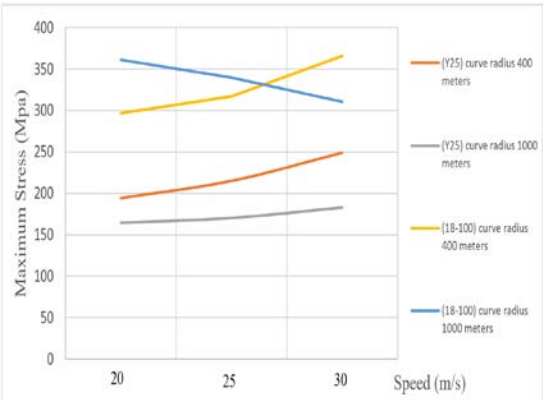

Figure 12. Average stress applied to the Y25 bogie axle and 18-100 during passage through curves with radii of 400 and 1000 meters at speeds of 72, 90, and 108 kilometers per hour.

In the 400-meter curve, the forces in the X direction decrease in both the left and right wheels with the increase in speed; however, in the left wheel, the forces in the Y and Z directions increase, while in the right wheel, the forces in the Y and Z directions decrease. In the 1000-meter curve, the forces in the X, Y, and Z directions in the left wheel increase with the increase in speed, while in the right wheel, the forces in the Y and Z directions decrease.

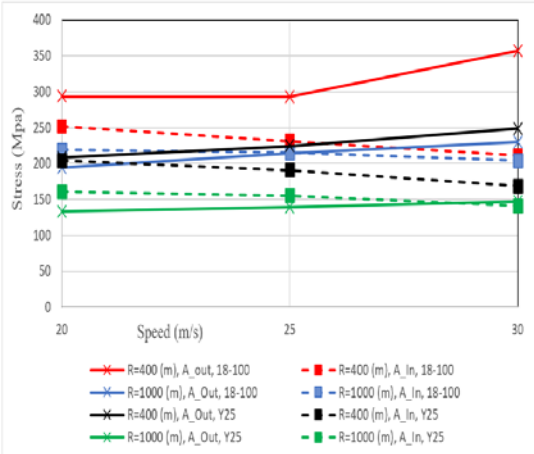

Figure 13. Average stress applied to area A

Note that the 44% higher stress in the 18-100 axle under similar vertical loading (and even 4% higher vertical load in Y25) is due to the combined effect of a sharper fillet geometry (higher Kt) and the presence of a non-negligible longitudinal force in the 18-100 bogie, as detailed in Section 3.1.

Due to the critical nature of the stresses in section A of the axles, the analytical graph for this area is presented for both bogies in the figure above. According to the chart, the stress applied to this section for the external axle increases with speed for both bogies and both curves, but the stresses applied to the internal axle show a decrease.

We also reviewed the literature of studies closely related to the topic and compared them to our research.

By studying the research conducted by Tuna and colleagues [3], which looked into wheel wear and rolling contact fatigue during curve passage, it is established that the forces applied to the front wheel and axle are higher than those at the rear, as well as the forces applied to the external axle being higher than those on the internal axle, as we reached in this research according to the axle analysis.

According to the studies and experiments conducted by Berta and colleagues [6], which examined the effects of scale on fatigue limits and crack growth rates for high-strength steel used in high-speed railway axles, a summary of fatigue strength (in terms of stress range for a 90 percent survival probability) for several categories of steel has been presented by evaluating the fatigue of railway axles. This summary reveals a systematic gap between the fatigue resistance of the material, with an average value of 510 MPa, and the fatigue strength of the axle based on the maximum applied stress, which has an average value of 380 MPa. According to our results in this study, the maximum average stress occurs at a curve of 400 meters and a speed of 108 km/h, reaching 357.57 MPa in the external axle 18-100 in section A, indicating the proximity of our results to theirs.

3.3. Parametric Effects

Analysis of stress variations with operational parameters revealed:

• Speed Influence: Stress increased by 15.4% (18-100) and 15.7% (Y25) when speed increased from 90 to 108 km/h on a 400 m curve.

• Curve Radius Effect: Transition from 1000 m to 400 m curve radius increased stresses by 21.8% (18-100) and 18.3% (Y25) at 72 km/h.

• Axle Position: Outer axles consistently experienced 40-60% higher stresses compared to inner axles.

3.4. Comparative Performance Assessment

The comprehensive stress analysis demonstrates that the Y25 bogie axle exhibits superior stress performance across all tested conditions. This advantage stems from its structural configuration and suspension characteristics, which better accommodate the geometric constraints of curve negotiation. The findings align with operational observations of improved Y25 performance in curved track sections and provide quantitative validation for its structural advantages.

The maximum stress value observed for the 18-100 axle (357.57 MPa) approaches the fatigue strength limits reported in the literature for high-strength railway steels, underscoring the importance of rigorous inspection and maintenance protocols for this bogie type [12]. In contrast, the lower stress levels in the Y25 axle suggest a potentially longer fatigue life under similar operating conditions. The comparative trends observed in this study find support in recent field measurements and simulation comparisons for different freight wagon bogies on small-radius curves [17], which similarly highlight significant performance variations between bogie types.

It should be noted that the reported 30% stress advantage of the Y25 bogie over the 18-100 bogie is derived under the assumption of rigid carbody and nominal pivot friction. The actual performance difference might vary with operating conditions, but the qualitative superiority of the Y25 design remains supported by independent literature.

4. Conclusion

Throughout the lifespan of a bogie, the axle experiences various loading conditions, with the most challenging being the train's passage through a curve. The stability and curve negotiation theories described above are still in use. These theories, formulated and adapted through modern computational methods, form the basis of the elements used in existing standards within simulation software, which is regularly utilized for the design and analysis of

railway vehicles. Minor fluctuations observed in some data points (e.g., a 0.2% stress reduction at 90 km/h compared to 72 km/h) are within the numerical error of the simulation and do not affect the prioritisation of critical conditions.

This study successfully conducted a comparative analysis of the stress states in the axles of Y25 and 18-100 freight bogies during curve negotiation. By integrating MBD simulations with FEA, the research quantified the impact of curve radius and vehicle speed on axle stress distributions. The key findings can be summarized as follows:

1. The fillet region at the axle journal-wheel seat intersection (Section A) represents the critical location for stress concentration, with maximum stresses consistently occurring on the outer axle. The stress on the outer axle's critical section (A) increased with speed for both bogies and curve radii, while the stress on the inner axle generally decreased.

2 .The Y25 bogie axle demonstrates superior performance with 30% lower maximum stress (248.33 MPa) compared to the 18-100 bogie axle (357.57 MPa) under identical severe operating conditions (400 m curve at 108 km/h).

3 .Operational parameters significantly influence stress magnitudes, with decreasing curve radius and increasing speed producing substantial stress elevations (15.4-15.7% increase with speed elevation from 90 to 108 km/h on 400 m curves). This is attributed to the increased lateral and vertical forces on the outer wheel during curve negotiation.

4. The maximum stress value for the 18-100 axle approaches fatigue strength limits reported in literature for high-strength railway steels [12], highlighting the importance of rigorous inspection protocols for this bogie type. The methodological framework and comparative findings of this study contribute to the growing body of research on bogie dynamics and axle stress analysis [11, 16, 17], providing a basis for future design optimizations and safety assessments.

The findings align with prior research, confirming that the leading outer wheel experiences the most severe loading. The maximum stress value observed for the 18-100 axle is notably close to the fatigue strength limits reported in the literature for high-strength railway steels, underscoring the importance of rigorous inspection and maintenance protocols for this bogie type.

Based on these results, future work should focus on design optimizations to mitigate stress concentrations in the critical fillet region. Furthermore, as suggested in this study, the adoption of advanced composite materials for non-critical bogie components could offer a promising pathway to reduce overall bogie mass, thereby lowering inertial forces and extending the fatigue life of safety-critical components like the axle.

A limitation of this study is the omission of rotary bending effects in the FE analysis; future work should employ transient dynamic analysis or multi-step quasi-static loading with axle rotation to obtain more accurate absolute stress values.

Another limitation is the omission of the time-varying nature of longitudinal forces; the applied static equivalents cannot reproduce the alternating shear stresses that contribute to fatigue crack growth at the press-fit fillet.

The study does not include sensitivity analysis for carbody flexibility or center-pivot friction coefficient, which could affect the absolute stress values, particularly for the 18-100 bogie.

The lack of a full circumferential stress analysis at the fillet region prevents a complete characterization of the stress concentration factor for each axle geometry. Future studies should report polar plots of stress vs. angular position to enable precise geometric optimization.

Declaration of Conflicting Interests

The author(s) declared no potential conflicts of interest with respect to the research, authorship, and/or publication of this article.

References

[1] K. Knothe, S. Stichel, Rail vehicle dynamics, Springer, Heidelberg, New York, (2017).

[2] P.T. Torstensson, J.C. Nielsen, Simulation of dynamic vehicle–track interaction on small

radius curves, Vehicle System Dynamics, Vol.49, No.11, (2011), pp.1711-1732.

[3] J. Tunna, J. Sinclair, J. Perez, A review of wheel wear and rolling contact fatigue, Proceedings of the Institution of Mechanical Engineers, Part F: Journal of Rail and Rapid Transit, Vol.221, No.2, (2007), pp.271-289.

[4] K. Wang, C. Huang, W. Zhai, P. Liu, S. Wang, Progress on wheel-rail dynamic performance of railway curve negotiation, Journal of traffic and transportation engineering (English edition), Vol.1, No.3, (2014), pp.209-220.

[5] X. Wu, M. Chi, P. Wu, Influence of polygonal wear of railway wheels on the wheel set axle stress, Vehicle System Dynamics, Vol.53, No.11, (2015), pp.1535-1554.

[6] S. Beretta, A. Ghidini, F. Lombardo, Fracture mechanics and scale effects in the fatigue of railway axles, Engineering fracture mechanics, Vol.72, No.2, (2005), pp.195-208.

[7] M. Madia, S. Beretta, U. Zerbst, An investigation on the influence of rotary bending and press fitting on stress intensity factors and fatigue crack growth in railway axles, Engineering Fracture Mechanics, Vol.75, No.8, (2008), pp.1906-1920.

[8] K. Hirakawa, K. Toyama, M. Kubota, The analysis and prevention of failure in railway axles, International journal of fatigue, Vol.20, No.2, (1998), pp.135-144.

[9] K. Knothe, A. Theiler, S. Güney, Investigation of contact stresses on the wheel/rail-system at steady state curving, In The Dynamics of Vehicles on Roads and on Tracks, CRC Press, (2021), pp.616-628.

[10] A.O. Shvets, Dynamic interaction of a freight car body and a three-piece bogie during axle load increase, Vehicle System Dynamics, Vol.60, No.10, (2022), pp.3291-3313.

[11] J. Tittel, M. Kepka, P. Heller, Static and dynamic testing of a bogie, IOP Conference Series: Materials Science and Engineering, Vol.723, No.1, (2020), p.012031.

[12] T. Makino, H. Sakai, C. Kozuka, Y. Yamazaki, M. Yamamoto, K. Minoshima, Overview of fatigue damage evaluation rule for railway axles in Japan and fatigue property of railway axle made of medium carbon steel, International Journal of Fatigue, Vol.132, (2020), p.105361.

[13] N. Bosso, M. Magelli, N. Zampieri, Dynamical effects of the increase of the axle load on european freight railway vehicles, Applied Sciences, Vol.13, No.3, (2023), p.1318.

[14] A. Avsievich, V. Avsievich, N. Avsievich, D. Ovchinnikov, A. Ivaschenko, Railway track stress–strain analysis using high-precision accelerometers, Applied Sciences, Vol.11, No.24, (2021), p.11908.

[15] X. Zhou, L. Jing, X. Ma, Dynamic finite element simulation of wheel–rail contact response for the curved track case, Transport, Vol.37, No.5, (2022), pp.357-372.

[16] R.C. Sharma, S. Palli, S. Bhardawaj, A review of wheel-rail dynamic behavior on curved tracks, International Journal of Vehicle Structures & Systems, Vol.15, No.1, (2023), pp.19-25.

[17] T.R. Loponen, R. Shaik, R. Varis, H. Luomala, P. Kolisoja, The Performance of Different Freight Wagon Bogie Types on a Small Radius Curve–Comparison of Field Measurements and Simulations, The Baltic Journal of Road and Bridge Engineering, Vol.19, No.4, (2024), pp.1-27.